Can Tho University Journal of Science
website: sj.ctu.edu.vn

FABRICATION AND CHARACTERIZATION OF GRAPHENE/GRAPHENE OXIDE BASED POLY (VINYL ALCOHOL) NANOCOMPOSITE MEMBRANES FOR PERVAPORATION DEHYDRATION OF ETHANOL

Nguyen Huu Hieu, To Lan Anh and Ngo Nguyen Phuong Duy
Faculty of Chemical Engineering, Ho Chi Minh City University of Technology, Vietnam

ARTICLE INFO

Received date: 25/01/2016
Accepted date: 08/07/2016

KEYWORDS

Graphene, graphene oxide, PVA, nanocomposite, membrane, pervaporation, dehydration, ethanol

ABSTRACT

Graphene (reduced graphene oxide-rgo) or graphene oxide (go)/poly(vinyl alcohol) (pva) nanocomposite membranes were fabricated by solution-casting method. The effects of additive content on the pervaporation (pv) performance of membranes were investigated. The membrane characterizations were performed by fourier-transform infrared spectroscopy, differential scanning calorimetry, x-ray diffraction, and transmission electron microscope. The characterized results indicated that thermal stability and pv performance of nanocomposite membranes were improved compared to the neat pva membrane. In comparison with neat pva, rgo/pva membrane showed a high selectivity of 51.2, but low permeate flux of 0.056 kg.m^{-2}h^{-1}); and go/pva exhibited an acceptable selectivity of 34.9, however equivalent permeate flux of 0.120 kg.m^{-2}h^{-1}

Cited as: Hieu, N.H., Anh, T.L. and Duy, N.N.P., (2016). Fabrication and characterization of graphene/graphene oxide based poly (vinyl alcohol) nanocomposite membranes for pervaporation dehydration of ethanol. Can Tho University Journal of Science. Special issue: Renewable Energy: 36-45.

1 INTRODUCTION

Pervaporation (PV) is an important membrane process for the separation of azeotropic mixtures, close-boiling systems, isomeric or heat-sensitive compounds. The popular applications of PV process are dehydration of alcohols and other organic solvents (Kaminski, 2008; Nguyen and Dang, 2009). This technique has advantages such as simplicity, no separating agents or chemicals required, save energy, and minimal environmental impact. Herein, instead of the physicochemical properties of components being separated and those of the mixture, the separation efficiency in PV is mainly based on the membrane properties and process conditions. This allows azeotropic mixtures to be separated more readily in PV than in the case of distillation. Moreover, in PV, the mixture to be separated doesn't need to be boiled and it is, hence, possible to utilize low-grade heat. As being distinct from distillation, which needs multiple evaporation of the entire mixture, PV consumes energy only for permeat evaporation. PV generally also doesn't need any extra reagents as azeotropic and extractive distillation, extraction or other methods employing extra chemicals… Thus, PV process also doesn't need subsequent recovery of these chemicals which complicates the separation of technology (Kaminski, 2008; Baker, 2014). Accordingly, PV is considered as a suitable separation technology for ethanol dehydration.

The PV membrane performance is expressed in terms of permeate flux (J – kg/m^{2}h), selectivity (α), and pervaporation separation index (PSI - kg/m^{2}h) (Tan *et al.*, 2001; Ver de Bruggen and Luis, 2015):

$$J = \frac{1}{A}\frac{\Delta W}{\Delta t} \quad (1)$$

$$\alpha = \frac{y_{H_2O}/y_{C_2H_5OH}}{x_{H_2O}/x_{C_2H_5OH}} \quad (2)$$

$$PSI = J(\alpha - 1) \quad (3)$$

where ΔW (kg) is the weight of permeate during the experimental time Δt (h), A (m^2) is the effective membrane area; and x, y are the mass fraction of either water or ethanol in the permeate and the feed, respectively. The pervaporation separation index is originally defined to measure the separation ability of a membrane, the higher PSI value the better separation ability. In case of PSI = 0, membrane has no selectivity (α = 1) or no pemeation (J = 0).

Poly(viny alcohol) (PVA) membranes have proved to be an ideal polymer for fabricating hydrophilic membranes because of their polar, low cost, and good membrane-forming properties in dehydration of ethanol by PV. However, PVA membranes often perform poorly in PV due to the swelling in water and the decline of the stability at high temperature, results in both an increase in solubility and diffusivity of ethanol, and consequently lowers the permselectivity. In this respect, improvement in the PV performance has been achieved by adding inorganic particles as nanofillers into the polymer matrix to form composite membranes. Such nanocomposite membranes have both forming properties of the polymer and physicochemical stability of the inorganic particles (Wang *et al.*, 2013).

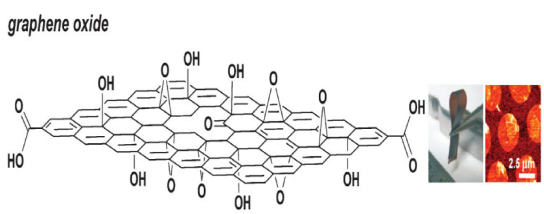

Fig. 1*:* Structural model of GO

Graphene oxide (GO) is product of oxidation and exfoliation of graphite (Gi). The structure of GO contains functional groups such as: epoxy (–O–), hydroxyl (–O–H), cacboxyl (–COOH) and cacbonyl (–C=O), as shown in Figure 1 (Compton *et al.*, 2010).

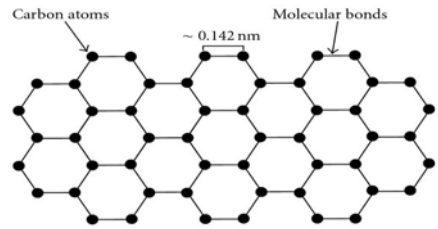

Fig. 2: Structural model of rGO

Graphene (reduced graphene oxide-rGO) is single layer of Gi containing sp^2-bonded carbon atoms arranged in hexagon to form 2D one-atom-thick sheet. Structure of rGO is shown in Figure 2 (Novoselov *et al.*, 2012).

In comparison with GO, rGO has fascinating properties such as super-mechanical, electrical and thermal properties (Novoselov *et al.*, 2012). Meanwhile, GO can be well dispersed at the individual-sheet level in aqueous solution because of its numerous oxygen-containing functional. Moreover, GO and rGO are well-known as promising fillers in membrane technology. The single layer GO or rGO with nano-size can be well dispersed in polymer matrix and improve properties of nanocomposite membrane. Interestingly, the appearance of GO or rGO will restrict the movement of PVA chains, which leads to increase the mechanical properties and reduce swelling. On the other hand, 2D-layer structures of GO and rGO contribute to prevent the permeation of large molecules throughout the membrane, increasing the selectivity (Wang *et al.*, 2011; Baker, 2014).

Accordingly, in this study, PVA nanocomposite membranes with different fillers (GO or rGO) were fabricated by solution-casting method (Yang *et al.*, 2010). The effect of GO or rGO contents on PV performance as well as morphology, structure, and properties of the nanocomposite membranes were investigated.

2 MATERIALS AND METHODS

2.1 Materials

PVA (molecular weight and the degree of saponification were 80,000 and > 98 %, respectively), sulfuric acid (98 wt%), sodium nitrate (99 wt%), hydrogen peroxide (30 wt%), hydrazine hydrate (35 wt%), and MA (99 wt%) were purchased from Xilong Chemical, China. Graphite (particle size: <

50 µm, density: 20-30 g/100 mL) was purchased from Sigma Aldrich, Germany. Potassium permanganate (> 99.5 wt%) and ethanol (96 vol%) were purchased from ViNa Chemsol, Vietnam.

2.2 Nanocomposite membrane preparation

Graphite oxide (GiO) was synthesized by chemical oxidation modified Hummers' method (Novoselov *et al.*, 2012). At first, 0.5 g of GiO was mixed with 500 mL of deionized water and sonicated for 12 h to exfoliate into GO. The obtained GO was centrifugated to remove the aqueous solution. And then, wet GO was finally washed with deionized water until pH=6, and dried at 60°C for 24 h.

Next, rGO was obtained via chemical reduction from GO. Accordingly, 0.1 g of GO was added into 100 mL of deionized water to obtain GO suspension. And then, 5 mL of hydrazine solution was added to 100 mL GO suspension and stirred for 30 minutes. The aqueous dispersion was sonicated for 4 h. Similarly to produce GO above, rGO was obtained after centrifugation, washing with deionized water and drying at 60°C for 24 h.

Nanocomposite membranes were prepared as follows: 0.05 g of GO or rGO was mixed with 500 mL of deionized water and sonicated for 24 h to obtain GO or rGO suspension. The nanocomposite membranes were fabricated by solution-casting method. Dried PVA (1.0 g) was dissolved in 100 mL deionized water and heated at 90°C to form aqueous PVA solution. Then, the PVA solution was mixed with certain amounts of GO or rGO suspension to be obtained by different GO/PVA or rGO/PVA ratios of 0.1, 0.2, 0.3, 0.4, and 0.5 wt% with respect to the weight of PVA. The mixture was stirred in 1 h and sonicated for 45 minutes. The obtained homogeneous solutions were casted in petry disk and dried at room temperature for 24 h to form membranes. After that, membranes continued to be dried at 100°C in 3 h to constant weight. A series of GO/PVA and rGO/PVA nanocomposite membranes with various GO or rGO contents were similarly prepared and named as 0.1GO/PVA, 0.2GO/PVA, 0.3GO/PVA, 0.4GO/PVA, 0.5GO/PVA or 0.1rGO/PVA, 0.2rGO/PVA, 0.3rGO/PVA, 0.4rGO/PVA, and 0.5rGO/PVA, respectively.

2.3 Pervaporation experiments

The PV system used in this study as illustrated in Figure 3. The PV dehydration of ethanol was carried out as follows: 1 L of 80 wt% ethanol feed solution was heated up to 50°C and circulated through the membrane module from the feed tank. Membrane was placed on a stainless steel screen support in the module with effective membrane area of 28.3 cm^2. During the experiment, the pressure at the downstream side was kept at -100 KPa by a vacuum pump. The permeate vapor was condensed in cold trap at -20°C. For each experiment, the operating time was 2 h to ensure that a steady state was reached. The collected permeate in cold trap was weighted to calculate the permeate flux and measured the concentration by a refractometer to determine the selectivity.

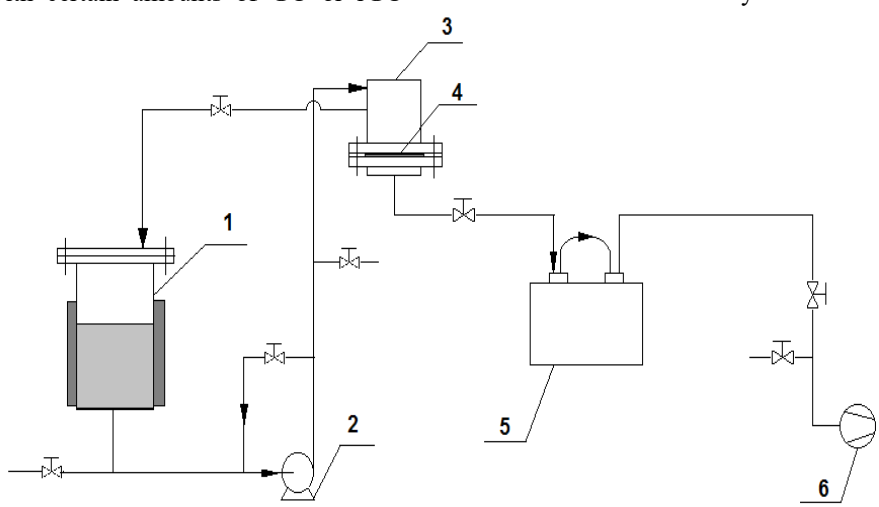

Fig. 3: Schematic diagram of PV system

1. Feed tank 2. Mettering pump 3.Membrane module 4. Membrane 5. Cold trap 6. Vacuum pump

2.4 Characterization

Fourier-transform infrared spectroscopy (FTIR) spectra were obtained in the range of wavenumber from 4000 to 500 cm^{-1} during 64 scans on Alpha–E Brucker (Bruker Optik GmbH, Ettlingen, Germany) spectrometer. Differential scanning calorimetry (DSC) was performed with DSC-1 (Mettler Tolado, America) differential scanning calorimeter. X-ray diffraction (XRD) patterns were obtained by Advanced X8, Bruker (German) with λ = 0,154 nm, step of 4°/minute from 10° to 50°. Atomic force microscopy (AFM) measurements were performed on an AFM Nanotec Electronica by casting powder dispersion onto freshly cleaved mica substrates and drying under ambient condition. Transmission electron microscope (TEM) images were taken by JEM-1400 machine with an accelerating voltage of 100 KV.

All measurements were carried out under 25°C and relative humidity of 30%.

3 RESULTS AND DISCUSSION

3.1 The dispersion of GO or rGO into PVA membrane

XRD is an effective method to characterize crystalline properties of nanocomposite. As shown in the Figure 4, the peak of neat PVA appeared at 2θ = 19.6°. However, the XRD patterns of GO/PVA and rGO/PVA nanocomposite membranes only showed the PVA diffraction peak. XRD results demonstrated a well-dispersing of the GO or rGO nanosheets into the PVA matrix. Hereby, the broad peak in GO or rGO disappeared in the composites, suggesting the disorder and loss of structure regularity of GO and rGO at 2θ = 9-11° and 21-26°, respectively. Moreover, after adding GO into PVA, the intensity of the diffraction of PVA decreased strongly in comparison to that of rGO. Such effect was ascribed to stronger interfacial interactions between GO and PVA matrix through the hydrogen bondings. These interactions probably restricted the capability of the matrix chains to form large crystalline domains and leaded to decline crystallinity of the GO/PVA (Zhao *et al.*, 2010; Zhou *et al.*, 2010; Wang *et al.*, 2011; Kang *et al.*, 2014).

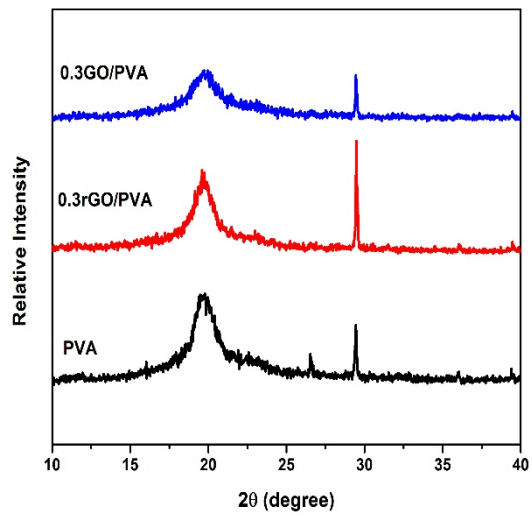

Fig. 4: XRD patterns of PVA, 0.3GO/PVA, and 0.3rGO/PVA

AFM image and height profiles for GO and rGO as shown in Figures 5 and 6. AFM results confirmed that GO and rGO were successfully synthesized which the average thickness of the obtained GO and rGO layers were found to be 0.913 nm and 0.921 nm, respectively.

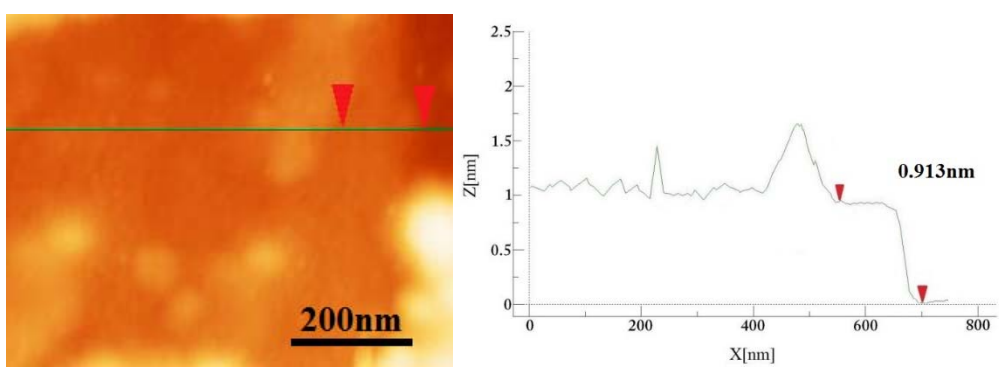

Fig. 5: AFM image and height profile of GO

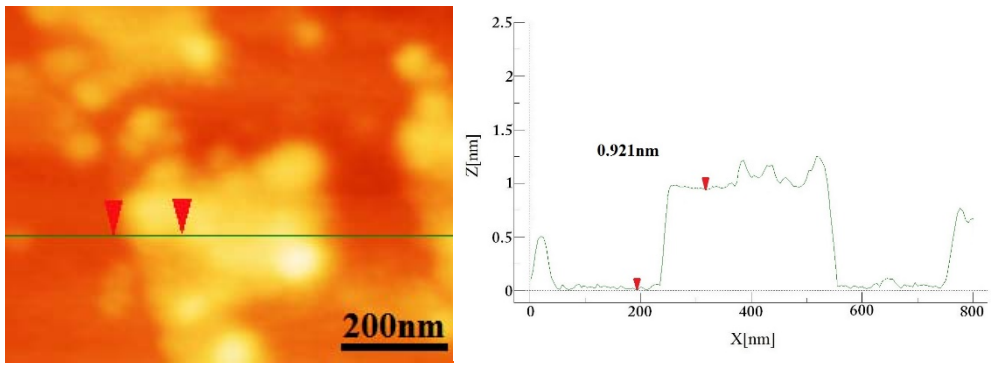

Fig. 6: AFM image and height profile of rGO

In order to evaluate the dispersion of GO and rGO in the PVA matrix, the ultrathin sections of nanocomposite membrane products were observed *via* Figures 7 (a) and 8 (a), which show the TEM images of 0.3GO/PVA and 0.3rGO/PVA, respectively. Apparently, a homogeneous dispersion and alignment of GO or rGO in PVA that obtained dark lines with the average thickness of 24-39 nm. Nevertheless, a little bit amounts of GO or rGO tended to restack together by Val der Waals forces that were observed in Figures 7 (a) and 8 (a). These effects mainly caused PVA crystallinity to be disrupted that was evident from XRD pattern above (Figure 4).

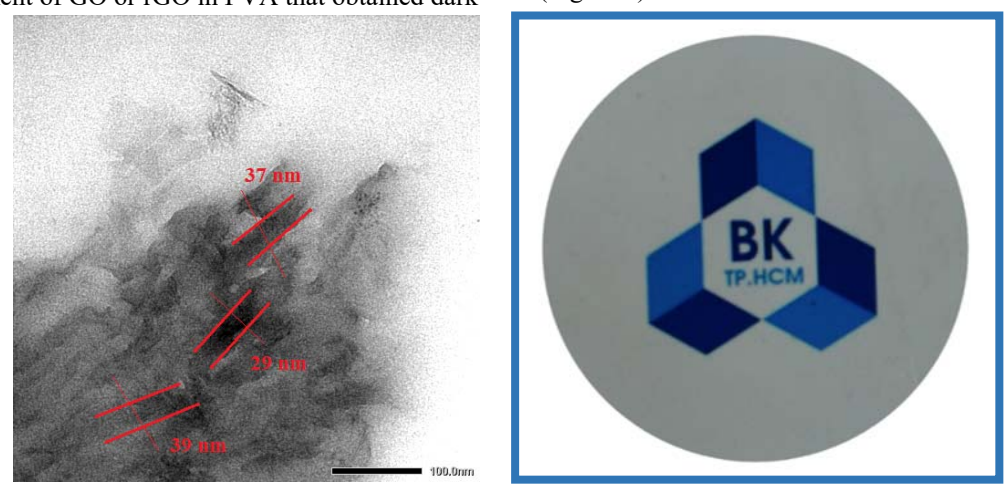

(a) **(b)**

Fig. 7: (a) TEM image and (b) photograph of 0.3GO/PVA membrane

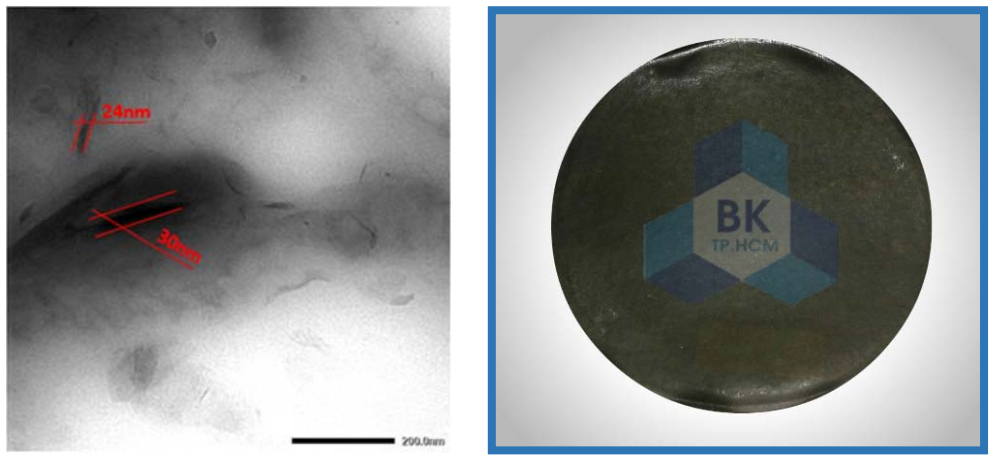

(a) **(b)**

Fig. 8: (a) TEM image and (b) photograph of 0.3rGO/PVA membrane

3.2 Interaction of GO or rGO nanosheets and PVA in nanocomposite membranes

Figure 9 shows FTIR spectra of PVA, 0.3rGO/PVA, and 0.3GO/PVA. As seen in the Figure 9, the absorptions at 3550 cm^{-1}- 3200 cm^{-1}, 2840 cm^{-1}-3000 cm^{-1}, and 1145 cm^{-1} are typical to the presence of –O–H, $–CH_2–$ (symmetric and asymmetric) and –C–O groups, respectively, of PVA matrix (Mansur *et al.*, 2008; Hossain *et al.*, 2014; Shuai *et al.*, 2015). Compared to neat PVA and GO, the spectrum of GO/PVA exhibited the enhancement of the –C=O stretching peak at 1741 cm^{-1} and the increase in the –O–H and –C–O stretching vibration, which can be identified as the presence of hydrogen bonding interactions between oxygen-containing functional groups of GO and the hydroxyl groups on PVA molecular chains, and the forming of free hydroxyl groups (Shuai *et al.*, 2015).

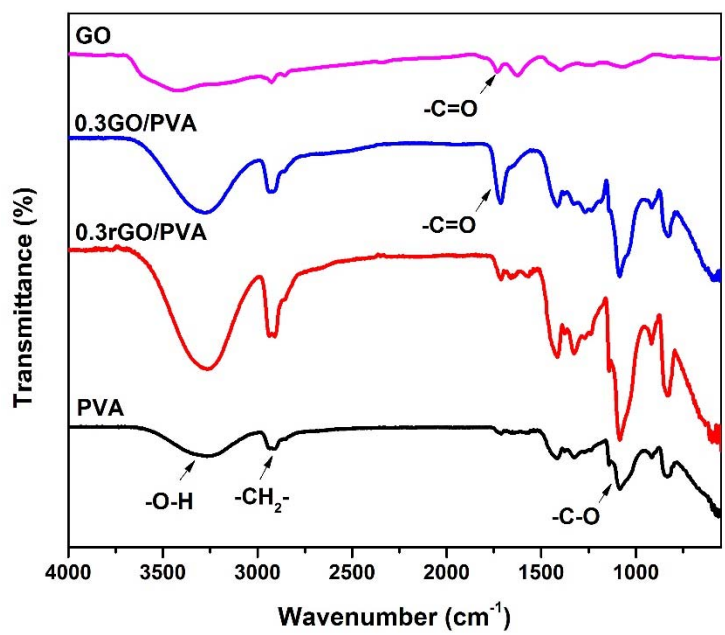

Fig. 9: FTIR spectra of PVA, 0.3GO/PVA, and 0.3rGO/PVA

Meanwhile, as non-interactions between rGO and PVA, rGO nanosheets were quite difficult to disperse into PVA matrix. Therefore, they could be restacked together and disrupted intermolecular hydrogen bonds between –O–H groups in PVA chains to form a large amount of free –O–H groups then. As a reason, –O–H and –C–O stretching peaks enhanced significantly. These results indicated that GO could disperse readily into PVA compared with that of rGO.

3.3 Thermal stability of nanocomposite membranes

DSC results illustrated in Figure 10. As it is reflected from Figure 10 and Table 1, when GO or rGO nanosheets were presented in the membranes, T_g which corresponded with thermal properties of the membranes is improved. In addition, GO/PVA showed a lower T_g than that of rGO/PVA. This due to the presence of GO or rGO, the PVA molecular chains were more stable under thermal condition. However, GO surface had many of oxygen-containing groups, which were easy to be decomposed by thermal effect. Consequently, destroying of PVA crystalline structure occured that caused GO/PVA less thermal stability than rGO/PVA.

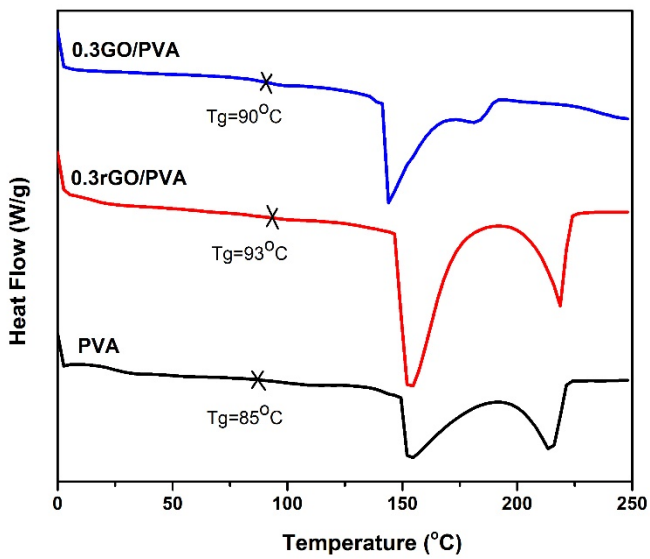

Fig. 10: DSC curves of PVA, 0.3GO/PVA, and 0.3rGO/PVA

Table 1: Glass trasition temperature (T_g) of membranes

Samples	T_g (°C)
PVA	85
0,3GO/PVA	90
0,3rGO/PVA	93

On the contrary, as a very thermally stable of carbon backbone, adding rGO into PVA that improved thermal stability for PVA membrane in comparison of GO (Bao *et al.*, 2011; Dhand *et al.*, 2013).

3.4 Pervaporation performance of nanocomposite membranes

Effects of different filler loading level on pervaporation performance of ethanol dehydration through membrane are depicted in Figures 11 and 12. Generally, neat PVA membrane showed selectivity (α = 21.4) and relative permeate flux (J = 0.10 kg.m^{-2}h^{-1}) at operating conditions. And after adding the filler with contents of 0.1-0.3 wt% of GO or rGO, nanocomposite membranes produced higher selectivity but lower permeate flux than that of neat PVA. However, the phenomenon showed in contrast when the filler contents were over 0.3 wt% of GO or rGO.

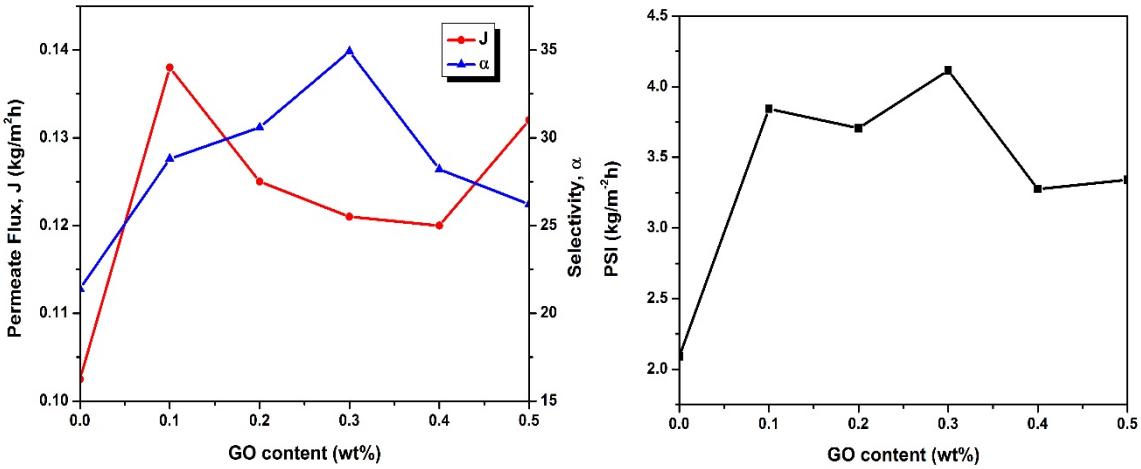

Fig. 11: Effect of GO loading contents on J, α, and PSI

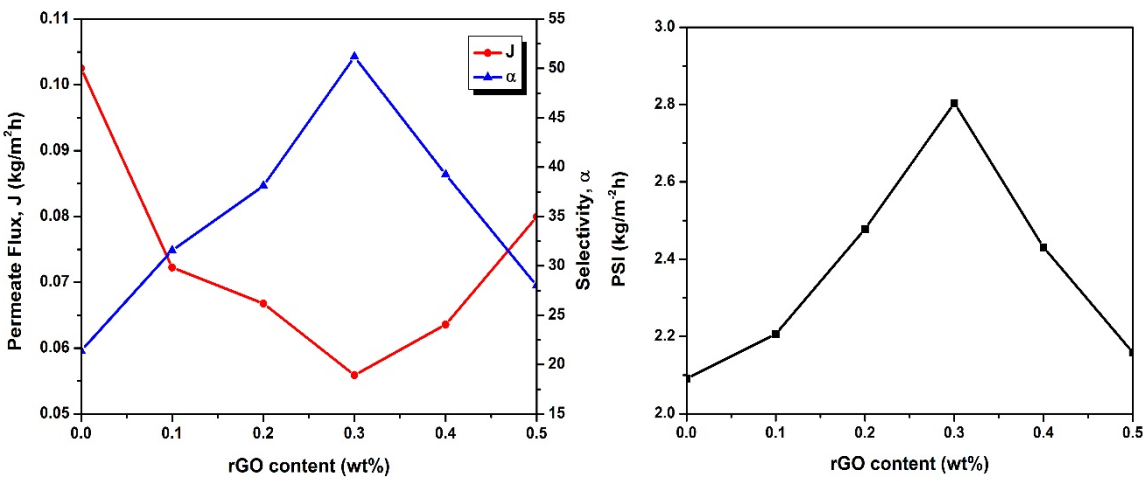

Fig. 12: Effect of rGO loading contents on J, α, and PSI

In particular, with adding GO into PVA matrix shown in Figure 11, at a low loading level (≤ 0.3 wt%), GO nanosheets were well-dispersed into and obtained stable structure with PVA chains. It was apparent that the selectivity of GO/PVA membrane increased and its permeate flux decreased. This can be explained due to a role of GO nanosheets were considered as molecular sieves that helped to reject large particles such as ethanol. Whereas, at GO loading level of over 0.3 wt%, GO interacted to PVA stronger and caused destroying crystallinity regions of PVA. Thus, permeate flux enhanced but selectivity dropped (Zhou *et al.*, 2010; Peng *et al.*, 2011; Kang *et al.*, 2014). The PSI results indicated that GO content of 0.3wt% exhibited the highest performance of ethanol dehydration with the equivalent selectivity of 34.9 and permeate flux of 0.120 $kg.m^{-2}h^{-1}$.

Likewise, rGO-based membranes also produced the higher selectivity and the lower permeate flux than neat PVA, as shown in Figure 12. This was in agreement with initial theoretical prediction of rGO nanosheets's effects after they were dispersed into PVA matrix. As a molecular sieve-like role of rGO nanosheets, the selectivity improved and the permeate flux decreased. When the loading content of rGO was over 0.3 wt%, the disruption of PVA crystallinity happened in mostly areas. As a result, it obtained holes in polymer structure which produced high permeate flux and low selectivity (Zhou *et al.*, 2010; Peng *et al.*, 2011; Wang *et al.*, 2011; Kang *et al.*, 2014). It could be assumed that the highest PSI value is at 0.3 wt% rGO content, which employed a double increasing in selectivity (α = 51.2) but a double drop in permeate flux (J = 0.056

$kg.m^{-2}h^{-1}$) in comparison with those of neat PVA membrane.

Generally, rGO/PVA membrane showed a high selectivity of 51.2, but low permeate flux of 0.056 $kg.m^{-2}h^{-1}$. Meanwhile, GO/PVA presented an acceptable selectivity of 34.9 and equivalent permeate flux of PVA membrane of 0.120 $kg.m^{-2}h^{-1}$. However, based on PSI – a parameter to evaluate performance of pervaporation, GO/PVA showed a better result (PSI = 4.12 $kg.m^{-2}h^{-1}$) than that of rGO/PVA (PSI = 2.80 $kg.m^{-2}h^{-1}$).

Table 2: Comparison of PV performance of the present membranes with literature for dehydration of 80 wt% ethanol feed solution

Membranes	J ($kg.m^{-2}h^{-1}$)	α	References
Zeolite clay/PVA	0.025÷0.035	45÷50	Ankudey and Zainudeen (2014)
1÷5 wt% Fullerenol/PVA	0.08÷0.130	36÷46	Penkova *et al.* (2014)
0.3GO/PVA	0.120	34.9	Present work
0.3rGO/PVA	0.056	51.2	Present work

Results of present work are compared with published data in literature as shown in Table 2. Evidently, the performance of GO/PVA and rGO/PVA nanocomposite membranes was improved in the selectivity and permeate flux.

4 CONCLUSIONS

GO/PVA and rGO/PVA nanocomposite membranes were prepared by solution-casting method. The effects of GO or rGO nanosheet contents on characteristics and PV performance of membranes were investigated with loading of 0.1-0.5 wt%. AFM results indicated that the successfully systhesized GO and rGO with the average thickness of 0.913 nm and 0.921 nm, respectively, were observed. TEM images revealed GO or rGO nanosheets dispersed into PVA matrix to the lines with the average thickness from 24 to 39 nm. Additionally, the XRD, FTIR, and DSC analyses also presented higher interaction and dispersion of GO nanosheets into PVA chains whereas rGO nanosheets indicated better stability of nanocomposite structure under thermal effects. The fabricated GO/PVA and rGO/PVA nanocomposite membranes exhibited a significant improvement in both of pervaporation of ethanol dehydration and thermal stability with 0.3 wt% GO or rGO loading compared to the neat PVA membrane. Accordingly, GO/PVA generally exhibited a better performance (PSI = 4.12 $kg.m^{-2}h^{-1}$) than that of rGO/PVA (PSI = 2.80 $kg.m^{-2}h^{-1}$).

ACKNOWLEDGEMENTS

This work was supported by Vietnam National University, Ho Chi Minh City through the TX2016-20-04/HĐ-KHCN project.

REFERENCES

Ankudey, E.G., Zainudeen, M.N., 2014. Pervaporative Separation of Ethanol-Water Mixture using Composite Membranes with Hydrophilic Zeolite fillers made from Ghanaian Clay deposits. International Journal of Scientific & Engineering Research. 5: 358-363.

Baker, R.W., 2014. Membrane technology and applications, Second Edition. England, 545 pages.

Bao, C.L., Guo, Y.Q., Song, L., Hu, Y., 2011. Poly(vinyl alcohol) nanocomposite based on graphene and graphite oxide: a comparative investigation of property and mechanism. J. Mater. Chem. 21: 13942-13950.

Bruggen, B.V., Luis, P., 2015. Pervaporation. *In*: E.S.Tarleton (Eds). Progress in Filtration and Separation. Academic Press. UK. pp. 101-154.

Compton, O.C., Nguyen, S.B.T., 2010. Graphene Oxide, Highly Reduced Graphene Oxide, And Graphene: Versatile Building Blocks For Carbon-Based Materials. Small Nano. 6: 711-723.

Dhand, V., Rhee, K.Y., Kim, H.J., Jung, D.H., 2013. A Comprehensive Review of GE Nanocomposite: Research Status and Trends. Journal of Nanomaterials. 2013: 1-14.

Dreyer, D.R., Park, S.J., Bielawski, C.W., Ruoff, R.S., 2010. The chemistry of graphene oxide. Chemical Society Reviews. 39: 228–240.

Hossain, U.H., Seidl, T., Ensinger, W.G., 2014. Combined *in-situ* infrared and mass spectrometric analysis of high-energy heavy ion induced degradation of polyvinyl polymers. Polymer Chemistry. 5: 1001-1012.

Kaminski, W., 2008. Renewable energy source-Dehydrated ethanol. Chemical Engineering Journal. 135: 95-102.

Kang, Q., Huybrechts, J., Van der Bruggen, B., Baeyens, J., Tan, T.W., Dewil, R., 2014. Hydrophylic membranes to replace molecular sieves in dewatering the bio-ethanol/water azeotropic mixture. Separation and Purification Technology. 136: 144-149.

Mansur, H.S., Sadahira, C.M., Souza, A.N., Mansur, A.A.P., 2008. FTIR spectroscopy characterization of poly (vinyl alcohol) hydrogel with different hydrolysis degree and chemically crosslinked with glutaraldehyde. Materials Science and Engineering C. 28: 539-548.

Nguyen, M.T., Dang, T.T.N., 2009. Pervaporation as a potential method for fuel ethanol production in Vietnam. *In*: Johor Bahru. Proceedings of South East Asian Technical Universities Consortium (SEATUC). 3rd SEATUC Symposium. Malaysia.

Novoselov, K.S., Fal'ko, V.I., Colombo, L., Gellert, P.R., Schwab, M.G., Kim, K., 2012. A roadmap for graphene. Nature. 490: 192-200.

Peng, F.B., Jiang, Z.Y., Hoek, E.M.V., 2011. Tuning the molecular structure, separation performance and interfacial properties of poly(vinyl alcohol)–polysulfone interfacial composite membranes, Journal of Membrane Science. 368: 26-33.

Penkova, A.V., Acquah, S.F.A., Dmitrenko, M.E., Chen, B.H., Semenov, K.N., Kroto, H.W., 2014. Transport properties of cross-linked fullerenol-PVA membranes. Carbon. 76: 446-450.

Shuai, C.J., Peng, P., Gao, C.D., Shuai, X., Xiao, T., 2015. Graphene oxide reinforced poly(vinyl alcohol): nanocomposite scaffords for tissue engineering applications. RSC advances. 5:25416-25423.

Tan, S.H., Ahmad, A.L., Nawawi, M.G.M., Hassan H., 2001. Separation of aqueous isopropanol through chitosan/poly(vinyl alcohol) blended membranes by pervaporation. IIUM Engineering Journal, 2: 7-12.

Wang, J.C., Wang, X.B., Xu, C.H., Zhang, M., Shang, X.P., 2011. Preparation of graphene/poly(vinyl alcohol) nanocomposites with enhanced machenical properties and water resistance. Polymer International. 60: 816-822.

Wang, N.X., Ji, S.L., Li, J., Zhang, R., Zhang, G.J., 2013. Poly(vinyl alcohol)-graphene oxit nanohybrid "pore-filling" membrane for pervaporation of toluene/n-heptane mixtures. Journal of Membrane Science. 455: 113-120.

Yang, X.M., Li, L., Shang, S.M., Tao, X.M., 2010. Synthesis and characterization of layer-aligned poly(vinyl alcohol)/graphene nanocomposites. Polymer. 51: 3431-3435.

Zhao, X., Zhang, Q.H., Chen, D.J., 2010. Enhanced Machenical Properties of Graphene-Based Poly(vinyl alcohol) Composites. Macromolecules. 43: 2357-2363.

Zhou, T.N., Chen, F., Tang C.Y., Bai, H.W., Zhang, Q., Deng, H., Fu, Q., 2010. The preparation of high performance and conductive poly(vinyl alcohol)/graphene nanocomposite via reducing graphite oxide with sodium hydrosulfite. Composites Science and Technology. 71: 1266-1270.